Effects of Dye Loading Conditions on the Energy Conversion Efficiency of ZnO and TiO_2 Dye-Sensitized Solar Cells

Tammy P. Chou, Qifeng Zhang, and Guozhong Cao*

Materials Science and Engineering, University of Washington, 302 Roberts Hall, Box 352120, Seattle, Washington 98195

Received: August 22, 2007; In Final Form: October 3, 2007

In this paper, we report the significant effects of dye loading conditions on the overall light conversion efficiency of zinc oxide (ZnO) film electrodes in dye-sensitized solar cells. A comparison of the ZnO film electrodes was also made with TiO_2 film electrodes prepared with similar dye loading conditions. It was found that using a higher and lower dye concentration requires a shorter and longer immersion time, respectively, for optimal sensitization of ZnO to obtain maximum efficiencies. A similar trend was found for the TiO_2 film electrode as well; however, smaller differences in the overall light conversion efficiencies were observed with varying dye concentration and immersion time. It was found that the chemical stability was an issue for the ZnO film electrodes but was not pertinent for the TiO_2 film electrodes. The film quality and structure of the ZnO film differed after prolonged immersion in high dye concentration, where the formation of N3 dye and Zn^{2+} aggregates and/or the deterioration of the ZnO colloidal spheres and nanoparticles on the surface may have occurred. On the other hand, the film quality and structure of the TiO_2 film was not appreciably affected by prolonged immersion in high dye concentration, where the nanoparticle structure was not affected.

Introduction

Zinc oxide (ZnO) has been explored as an alternative material in dye-sensitized solar cells. The use of ZnO as the semiconductor electrode instead of the typical TiO_2 semiconductor electrode has the greatest potential as an alternative material for improving the solar cell performance in dye-sensitized solar cells due to (1) ZnO having a band gap similar to that for TiO_2 at 3.2 eV,[1] and (2) ZnO having a much higher electron mobility ∼115−155 $cm^2/V{\cdot}s^2$ than that for anatase TiO_2, which has been reported to be $\sim 10^{-5}$ $cm^2/V{\cdot}s$.[3] In addition, the tailoring of the ZnO nanostructure during the processing step allows for the potential of easily varying the nanostructure through solution modification.

Baxter and co-workers[4−6] synthesized ZnO nanowires for the fabrication of the working electrode in dye-sensitized solar cells using metal−organic chemical vapor deposition (MOCVD) from zinc acetylacetonate hydrate vapor and oxygen gas. They also used a seeding method nucleated from ZnO nanoparticles using zinc nitrate hexahydrate and methenamine in deionized water to grow ZnO nanowires on transparent conductive substrates. With these techniques to form ZnO nanowires, overall light conversion efficiencies as high as 0.5% were achieved.

Law et al.[7] also fabricated ZnO nanowire-based dye-sensitized solar cells using a seeding method in aqueous solution containing zinc nitrate hydrate, hexamethylenetetramine, and polyethyleneimine, obtaining overall efficiencies as high as 1.2%. They further studied core−shell[8] structures combining their fabricated ZnO nanowire system with layers of TiO_2, resulting in a further increase in the overall light conversion efficiency to 2.25%.

Many other groups have also extensively studied ZnO in various hierarchically structured forms, including nanorods,[9] nanotubes,[10] core−shell nanostructures,[11] flower-like nanowires,[12] branched nanowires,[13] and needle-like nanowires,[14] and in various structures combining two materials,[15,16] but none have surpassed the 5%[17,18] overall light conversion efficiency obtained for ZnO nanoparticle films. Electrodes consisting of ZnO with a high surface area, in conjunction with a higher electron mobility than that for TiO_2, are thought to provide a promising means for improving the solar cell performance of dye-sensitized solar cells. However, the highest overall light conversion efficiency obtained for sensitized ZnO electrodes so far does not compare with the highest overall light conversion efficiency obtained for sensitized TiO_2 electrodes, which has shown to be ∼11%.[19−23]

One possible reason for the lower overall efficiency of ZnO is its stability, which has shown to be compromised in solvent-rich or acidic environments. It has been reported[24] that the dye adsorption behavior of ZnO is poor compared to TiO_2 due to the lower chemical stability of ZnO relative to the chemical stability of TiO_2. In addition, it has been reported[25] that the high acidity of the dye due to the presence of carboxylic acid binding groups can lead to dissolution of ZnO and precipitation of complexes consisting of the dye and Zn^{2+} ions, resulting in reduced overall electron injection efficiency by the excited dye. Although Quintana et al.[26] found that (1) the electron transport times and light intensity dependence was found to be similar for ZnO and TiO_2, (2) the electron lifetime was significantly higher in ZnO than that in TiO_2, and (3) the recombination rate for ZnO was lower than that for TiO_2, the performance of ZnO solar cells was lower than that of TiO_2 solar cells due to a lower electron injection efficiency and/or a lower dye regeneration efficiency attributed to the chemical instability of ZnO.

In an effort to determine the effects of dye loading on the stability of ZnO films, as compared to TiO_2 films, solar cells consisting of ZnO film electrodes sensitized in various dye concentrations for various immersion times were prepared and analyzed to compare the overall light conversion efficiency.

* Corresponding author. E-mail: gzcao@u.washington.edu.

10.1021/jp076724f CCC: $37.00
Published on Web 11/29/2007

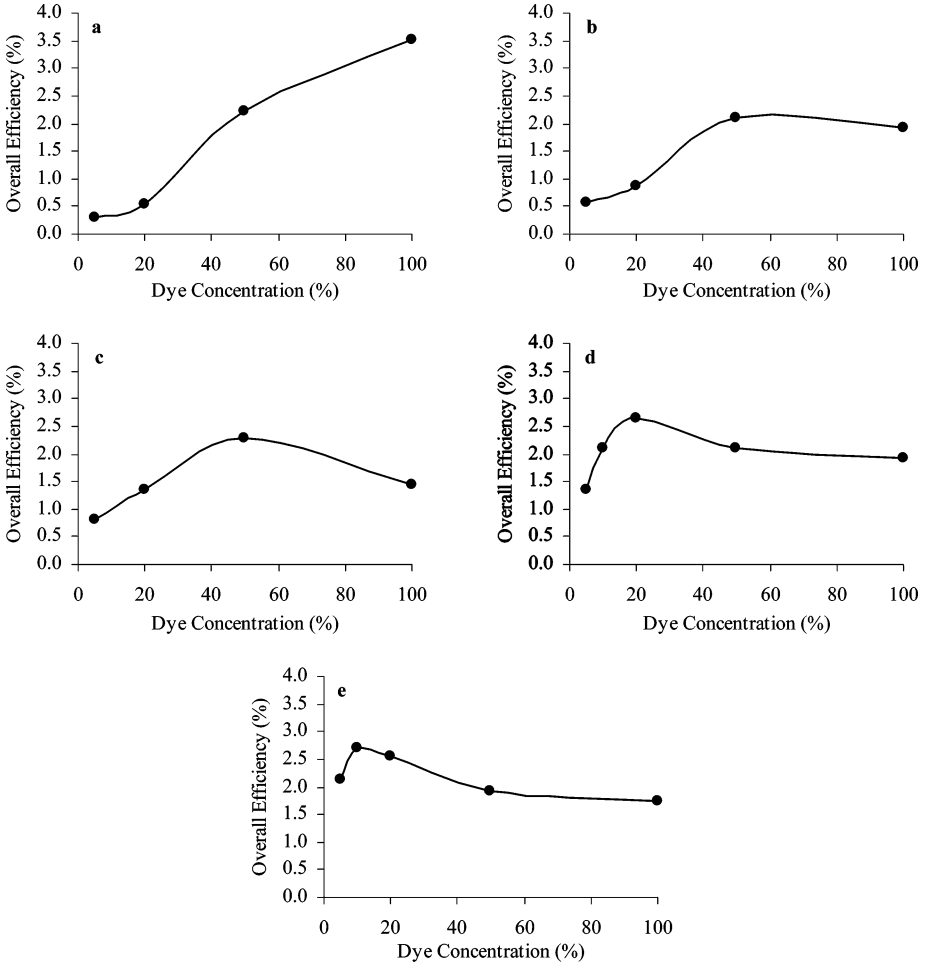

Figure 1. Sequence plots of the overall efficiency trends indicating the resultant efficiency as a function of dye concentration for immersion times of (a) 20, (b) 40, (c) 60, (d) 120, and (e) 180 min for the ZnO film electrodes. The highest point in each plot indicates the maximum overall conversion efficiency at the specified dye concentration and immersion time.

Additional comparisons were also made with TiO_2 film electrodes prepared in similar dye loading conditions. The ZnO films consist of primary colloidal spheres ~300 nm in diameter and secondary nanoparticles ~20 nm in diameter on the surface of the spheres, as previously reported.[27] By exposing this type of ZnO film structure to the sensitizer dye with varying concentrations for a wide range of immersion times, the resultant dye sensitization, the quality of the films, and the differences in the morphology of the colloidal spheres can be analyzed as a means to correlate the overall light conversion efficiency to the dye adsorption behavior, as well as the stability of the films.

Experimental Procedures

1. Fabrication of ZnO Colloidal Spheres. Zinc oxide (ZnO) solution was prepared from precursor materials of zinc acetate (98%, Alfa-Aesar, Ward Hill, MA), diethylene glycol (98%, Sigma-Aldrich, St. Louis, MO), and deionized water (DI H_2O). The ZnO solution was prepared by hydrolyzing 0.01mol of zinc acetate [$(CH_3CO_2)_2Zn$] in 100 mL of diethylene glycol [$(HOCH_2CH_2)_2O$], as described by Jezequel et al.[28] The reaction occurred when the mixed solution was heated under reflux to 160 °C for ~8 h. The as-synthesized solution was then placed in a centrifuge tube. The solution was centrifuged at a rate of ~1400 revolutions/min (rpm) for ~2 h. After centrifugation, the precipitation of ZnO colloids segregated to the bottom of the tube. Part of the supernatant was removed, and the colloids were then redispersed in ethanol by sonication for ~30 min. The resultant ZnO colloidal spheres were sealed and stored at room temperature. The colloidal spheres produced by this method are typically monodispersed with a diameter size of ~300 nm and consist of many secondary nanoparticles with a diameter of ~20 nm.

2. Fabrication of ZnO Films. Films consisting of ZnO colloidal spheres were fabricated on fluorine−tin−oxide (FTO, TCO10-10, R_s ~10 ohm/sq, Solaronix SA, Switzerland) coated glass substrates. To fabricate ZnO films, the substrates were first hydrolyzed in boiling DI H_2O at 90−100 °C for ~30 min. A few drops of the resultant ZnO colloidal spheres were placed onto FTO glass substrates. The films were then immediately heat treated at a temperature of 450 °C for 1 h, forming a layer of white film during the quick evaporation of the solvent. The thickness of the films varied from 2 to 10 μm, depending on the concentration of the colloidal spheres and the quantity added to the substrate surface.

3. Fabrication of TiO_2 Nanoparticles and Films. Nanoparticles of TiO_2 were obtained by hydrothermal treatment at 250 °C for 20 min, and films were prepared on FTO substrates for comparison, as previously described.[29]

4. Dye Loading of N3 Sensitizer. Before solar cell testing, the ZnO and TiO_2 films were sensitized with standard ruthenium-based red dye (N3), *cis*-bis(isothiocyanato)bis(2,2′-bipyridyl-4,4′-dicarboxylato)ruthenium(II) (Solterra Fotovoltaico SA,

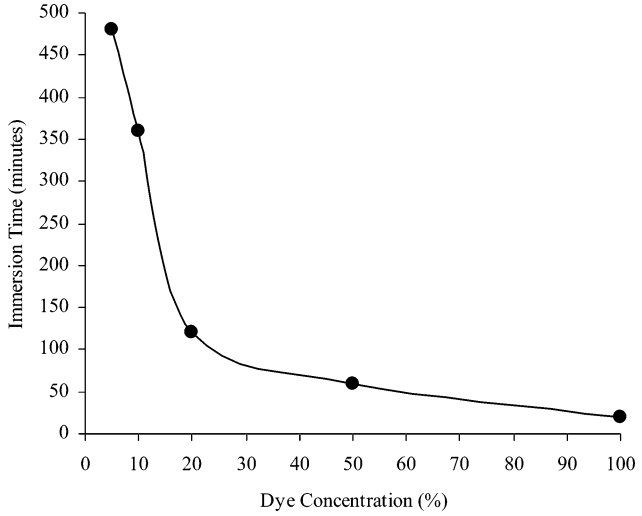

Figure 2. Plot of immersion time as a function of dye concentration at the point of maximum overall light conversion efficiency in each sequence plot shown in Figure 1. The combination of immersion time and dye concentration shown in the plot indicates the parameters necessary for obtaining the maximum overall light conversion efficiency in each case.

TABLE 1: Summary of Values Showing the Open-Circuit Voltage, Short-Circuit Current Density, and Overall Light Conversion Efficiency for ZnO Film Electrodes Sensitized in Various Concentrations for 20 min

N3 dye concn (%)	V_{oc} (mV)	J_{sc} (mA/cm^2)	V_{max} (mV)	J_{max} (mA/cm^2)	FF (%)	P_{max} (mW/cm^2)	P_{in} (mW/cm^2)	η (%)
100	670	10.9	420	8.35	48.1	3.51	100	3.51
50	660	7.75	400	5.57	43.6	2.23	100	2.23
20	540	1.91	360	1.49	52.0	0.54	100	0.54
5	510	1.15	350	0.82	48.9	0.29	100	0.29

Switzerland), with varying concentrations for various immersion times to determine the effect of dye loading on the overall light conversion efficiency of the films. The original 5×10^{-4} M N3 dye concentration in ethanol (100%) was modified to obtain 50%, 20%, 10%, and 5% concentrations through further dilution by the addition of various amounts of ethanol. In addition, the ZnO films were immersed in N3 dye for various times ranging from 20 min up to 3 h. An additional immersion time of 4 and 8 h was only performed at 10% concentration and 5% concentration, respectively, for the ZnO film. For comparison, similar dye loading concentrations were also performed on TiO_2 films. However, the TiO_2 films were immersed in N3 dye for different times ranging from 30 min up to 5 h.

5. Solar Cell Assembly. Colloidal liquid silver (Ted Pella Inc., Redding, CA) was placed at the electrical contacts to improve the contact points and allowed to cure for 30 min at room temperature. Sheets of weigh paper ~30−40 μm thick were cut into small pieces ~1 mm × 4 mm in dimension and used as spacers. A spacer was placed at each edge of the working electrode, and the counter electrode consisting of a Pt-coated silicon (Si) substrate with a Pt layer thickness of ~180 nm was placed on top, with the Pt-coated side of each Si substrate facing the working electrode. Each solar cell was held in place with two heavy-duty clips on opposite ends.

An iodide-based solution was used as the liquid electrolyte, consisting of 0.6 M tetrabutylammonium idodide (Sigma-Aldrich, St. Louis, MO), 0.1 M lithium iodide (LiI, Sigma-Aldrich, St. Louis, MO), 0.1 M iodine (I_2, Sigma-Aldrich, St. Louis, MO), and 0.5 M 4-tertbutyl pyridine (Sigma-Aldrich, St. Louis, MO) in acetonitrile (Mallinckrodt Baker, Phillipsburg, NJ). Right before analysis, drops of the liquid electrolyte were introduced to one edge of the sandwich, where capillary force was used to spread the liquid electrolyte in between the two electrodes. The light source was placed next to each solar cell device, allowing light to penetrate through the FTO back-contact to the dye adsorbed onto the film electrode.

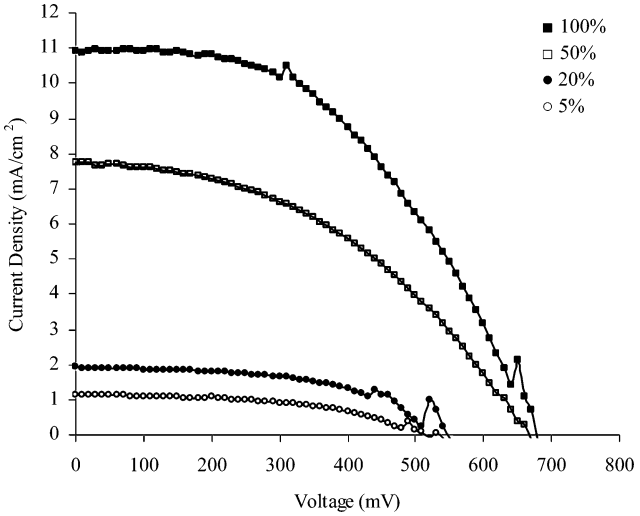

Figure 3. Plot comparing the $I-V$ behavior of ZnO electrode films sensitized in 100%, 50%, 20%, and 5% N3 dye concentrations for 20 min.

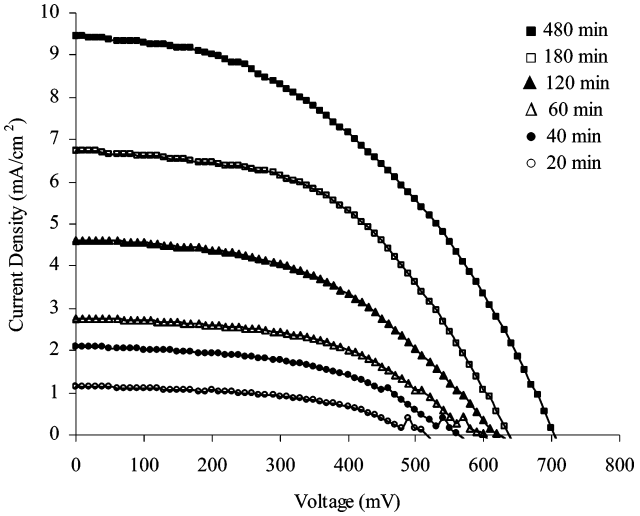

Figure 4. Plot comparing the $I-V$ behavior of ZnO electrode films sensitized in 5% N3 dye concentration for 20, 40, 60, 120, 180, and 480 min.

TABLE 2: Summary of Values Showing the Open-Circuit Voltage, Short-Circuit Current Density, and Overall Light Conversion Efficiency for ZnO Films Sensitized in 5% Concentration for Various Immersion Times

N3 dye immersion time (min)	V_{oc} (mV)	J_{sc} (mA/cm^2)	V_{max} (mV)	J_{max} (mA/cm^2)	FF (%)	P_{max} (mW/cm^2)	P_{in} (mW/cm^2)	η (%)
20	510	1.15	350	0.82	48.9	0.29	100	0.29
40	560	2.09	370	1.54	48.7	0.57	100	0.57
60	600	2.77	390	2.08	48.8	0.81	100	0.81
120	620	4.62	390	3.44	46.8	1.34	100	1.34
180	630	6.75	410	5.20	50.1	2.13	100	2.13
480	700	9.45	440	6.57	43.7	2.89	100	2.89

6. Analysis Techniques. Scanning electron microscopy (SEM) (JEOL JSM-5200, JEOL 840A, JSM-7000) was used to study the morphology of the ZnO and TiO_2 films. The films

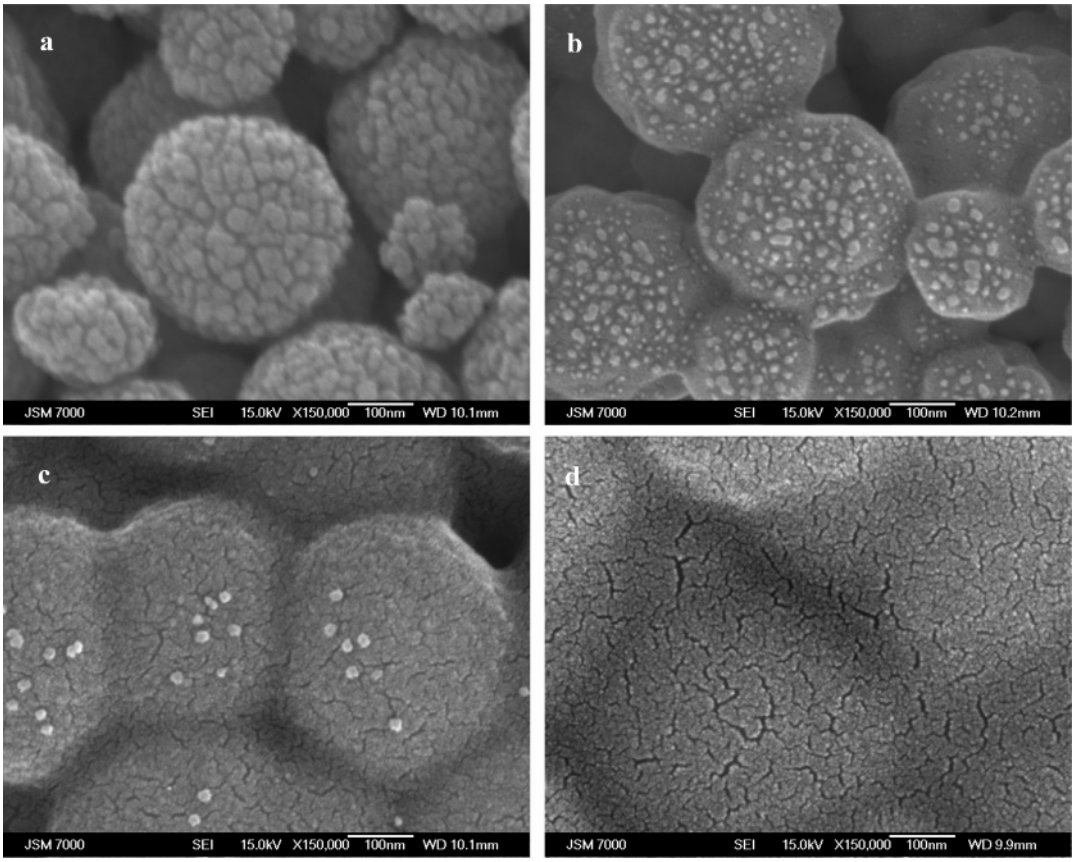

Figure 5. SEM images of ZnO film (a) before and (b−d) after sensitization in 100% N3 dye concentration for (b) 20 min, (c) 12 h, and (d) 24 h.

on FTO substrates were placed on an aluminum SEM stub, using a layer of silver paste for attachment. All samples were sputter-coated with a thin layer of Au/Pd or Pt prior to SEM observation for better imaging. The images were obtained at 15 kV from 1000× up to 150 000× magnification, depending on the sample.

Electrical characteristics and photovoltaic properties of each solar cell were measured using simulated AM1.5 sunlight illumination with 100 mW/cm^2 light output. An ultraviolet solar simulator (model 16S, Solar Light Co., Philadelphia, PA) with a 200 W xenon lamp power supply (model XPS 200, Solar Light Co., Philadelphia, PA) was used as the light source, and a semiconductor parameter analyzer (4155A, Hewlett-Packard, Japan) was used to measure the current and voltage. The intensity of the light source provided by the Xenon lamp was measured with a photometer/radiometer (PMA2200, Solar Light Co., Philadelphia, PA) connected with a full spectrum pyranometer (PMA2141, Solar Light Co., Philadelphia, PA). All the $I-V$ curves of the solar cells were obtained in the dark and under illumination, where a voltage range from −0.3 to 2 V was used during each measurement. The $I-V$ characteristics as a function of incident light intensity were used to obtain the open-circuit voltage (V_{oc}), short-circuit current density (J_{sc}), the maximum voltage point (V_{max}), and the maximum current density point (J_{max}). Multiple samples were tested for each nanoparticle film, resulting in reproducible results with slight deviations in the short-circuit current (∼±0.05 mA), open-circuit voltage (∼±10 mV), and the light conversion efficiency (∼±0.02%).

Results and Discussion

Solar cell analysis was performed on all the ZnO film electrodes sensitized in N3 dye with various concentrations for varying amounts of time to compare the sensitizer concentration and the immersion time to the resultant overall light conversion efficiency. It was found that at higher dye concentrations, a shorter immersion time is needed to obtain the highest overall light conversion efficiency. Or in other words, at lower dye concentrations, a longer immersion time is needed to obtain the highest overall light conversion efficiency. This can be better illustrated by looking at the sequence of efficiencies obtained for the ZnO film electrodes when sensitized for a specified time in a range of dye concentrations.

Figure 1 shows the efficiency trends at various concentrations for 20, 40, 60, 120, and 180 min. It is important to note that the plots only show the overall efficiency values of the ZnO film electrodes and that the corresponding short-circuit current density values is not indicated; however, it was found that the overall trend of the corresponding short-circuit current density values was similar to that of the overall efficiency plots in Figure 1. From the plots in Figure 1, it can be seen that the peak in the sequence plots, which represents the maximum overall efficiency, is shifted to a lower concentration when the immersion time is increased.

The ZnO film sensitized for 20 min in 100% dye concentration, as shown in Figure 1a, resulted in an efficiency of 3.51%. With a decrease in the dye concentration to 50%, the efficiency of the sensitized ZnO electrode decreased from 3.51% down to 2.23%. Further decreases in the dye concentration resulted in much lower efficiencies ranging from 0.54% down to 0.29%.

At 40 and 60 min immersion time, as shown in their respective plots in Figure 1, parts b and c, the ZnO film sensitized in 50% dye concentration resulted in the highest efficiency of 2.12% and 2.30%, respectively. A higher dye

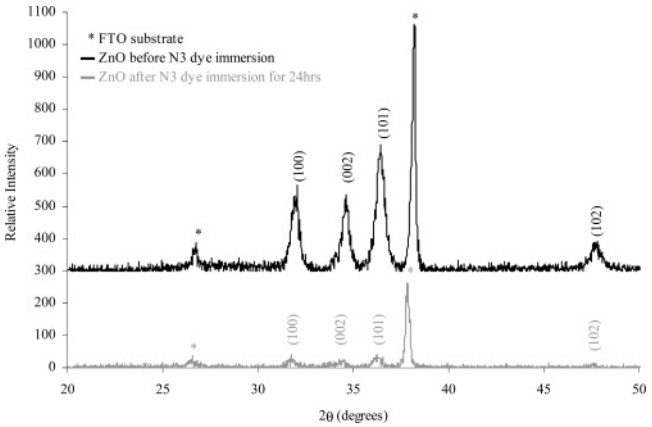

Figure 6. XRD plots of ZnO film before (black line) and after (gray line) sensitization in 100% N3 dye concentration for 24 h. The peaks (*) representing the FTO substrate are also shown.

concentration of 100% resulted in a lower efficiency of 1.93% and 1.43%, respectively; and a lower dye concentration than 50% resulted in much lower efficiencies ranging from 0.88% down to 0.57% and from 1.36% down to 0.81%, respectively.

In Figure 1d, the use of an immersion time of 120 min resulted in the highest efficiency for the ZnO film when sensitized in 20% dye concentration with a value of 2.66%. A higher and lower dye concentration than 20% resulted in lower efficiencies ranging from 2.11% down to 1.93% and 2.12% down to 1.34%, respectively.

From Figure 1e, at 180 min immersion time, the ZnO film sensitized in 10% dye concentration resulted in the highest efficiency of 2.70%. Higher concentrations than 10% resulted in lower efficiencies ranging from 2.57% down to 1.75%, and a lower concentration of 5% also resulted in a lower efficiency of 2.13%. It is also important to note that at 10% and 5% dye concentrations, an even higher efficiency is obtained at even longer immersion times. At 10% and 5% dye concentrations, the ZnO film immersed for 360 and 480 min, respectively, resulted in the highest efficiencies of 2.92% and 2.89%, respectively.

Furthermore, Figure 2 shows a complete plot of the immersion time necessary to adequately sensitize the ZnO film at specific concentrations for obtaining the maximum overall light conversion efficiency, as shown in Figure 1. The plot represents the immersion time as a function of dye concentration and also includes the 360 and 480 min immersion time for the 10% and 5% concentrations, respectively.

It can be seen that a lower dye concentration requires a longer immersion time, and a higher dye concentration requires a shorter immersion time. At 5% and 10% dye concentrations, an immersion time of 480 and 360 min is required for sufficient sensitization, respectively. At 20% dye concentration, an even shorter immersion time of 120 min is necessary for adequate film sensitization. With an increase in the dye concentration to 50%, the immersion time is cut in half to ~40−60 min to sufficiently sensitize the ZnO film. With a further increase in the dye concentration to 100%, the immersion time is further cut in half to 20 min to adequately sensitize the ZnO film. At 100%, 50%, 20%, 10%, and 5% dye concentrations, their respective immersion times of 20, 60, 120, 360, and 480 min were required to obtain their respective maximum overall light conversion efficiencies of 3.51%, 2.30%, 2.66%, 2.92%, and 2.89%.

A closer look at the solar cell $I-V$ behavior of the ZnO films sensitized in various concentrations for 20 min shows that a decrease in the N3 dye concentration resulted in a decrease in the short-circuit current density and, thus, a decrease in the overall light conversion efficiency. Table 1 summarizes the open-circuit voltage, short-circuit current density, and overall light conversion efficiency relative to the dye concentration at an immersion time of 20 min, found from Figure 3.

Figure 3 compares the $I-V$ behavior of the ZnO film electrodes immersed in various dye concentrations for 20 min. It can be seen that the short-circuit current density decreases with decreasing dye concentration when a short immersion time of 20 min is used. This shows that at high concentrations, a short immersion time of 20 min is sufficient for enough dye adsorption to occur to obtain high conversion efficiency, as shown from the larger short-circuit current density found at 100% concentration. However, at low concentrations, an immersion time of 20 min is insufficient for enough dye adsorption to occur, giving rise to incomplete surface coverage by the dye molecules, as evidenced by the lower short-circuit current density and lower light conversion efficiency found at 5% concentration. Insufficient surface coverage of the light-absorbing dye on the surface of the film would result in a reduction in the number of electron and electron−hole pairs generated after photon absorption, consequently decreasing the short-circuit current density and overall light conversion efficiency. It is also important to note that the variation of the open-circuit voltage is prevalent in dye-sensitized ZnO solar cells, which is thought to be due to its instability and reactivity with the N3 dye, as will be discussed later in this paper.

Taking a closer look at the low efficiency found at 5% concentration for 20 min, most likely due to insufficient surface coverage, the solar cell $I-V$ behavior of the ZnO electrode films sensitized in 5% dye concentration for various immersion times was compared. Figure 4 compares the $I-V$ behavior of the ZnO film electrodes immersed in 5% dye concentration for various immersion times. Table 2 summarizes the open-circuit voltage, short-circuit current density, and overall light conversion efficiency relative to the immersion time at 5% concentration, found from Figure 4.

Figure 4 shows that an increase in the immersion time in 5% dye concentration resulted in an increase in the short-circuit current density and, thus, an increase in the overall light conversion efficiency. This shows that at low concentrations, a long immersion time is necessary for enough dye adsorption to occur to obtain maximum overall conversion efficiency, as shown from the larger short-circuit current density found at 480 min. A longer immersion time in low dye concentrations allows for sufficient time for complete surface coverage by the dye molecules. This is evidenced by the increase in short-circuit current density and overall light conversion efficiency with increasing immersion time. Sufficient surface coverage of the light-absorbing dye on the surface of the film would result in a greater number of electron and electron−hole pairs generated after photon absorption, thereby increasing the short-circuit current density and overall light conversion efficiency.

A dye concentration of 5×10^{-4} M (equivalent to 100%) has been widely used for the sensitization of TiO_2 film electrodes used in dye-sensitized solar cells. In this case, a minimum of 12 h is used for complete dye adsorption on the TiO_2 surface. However, in the case of ZnO film, it was found that prolonged immersion in 100% dye concentration resulted in a decrease in the performance of the electrode when used in dye-sensitized solar cells. To further determine what effect immersion time in 100% dye concentration has on the ZnO electrode film, SEM analysis was performed.

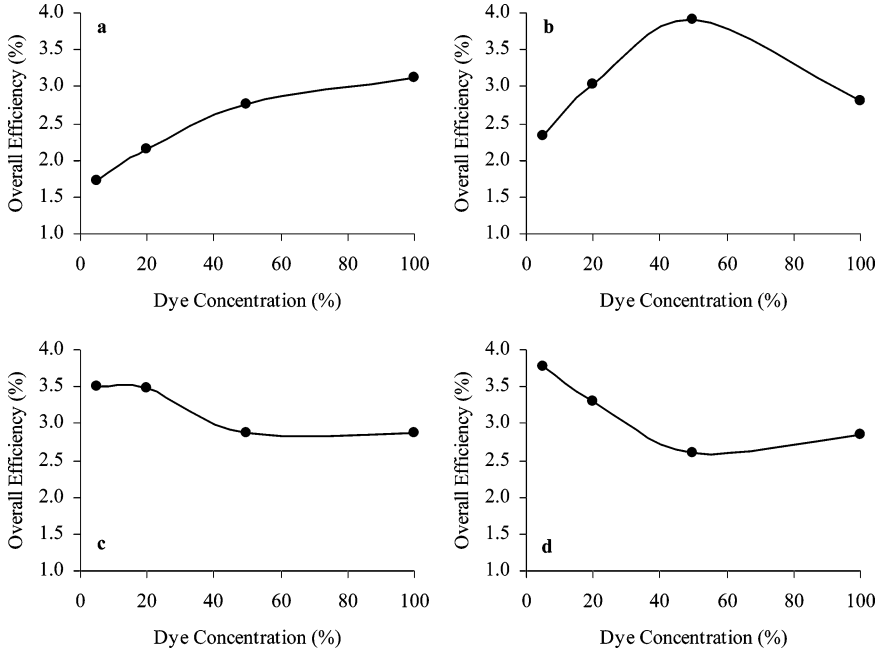

Figure 7. Sequence plots of the maximum overall efficiency trends indicating the resultant efficiency as a function of dye concentration for immersion times of (a) 30, (b) 60, (c) 180, and (d) 300 min for the TiO_2 film electrodes.

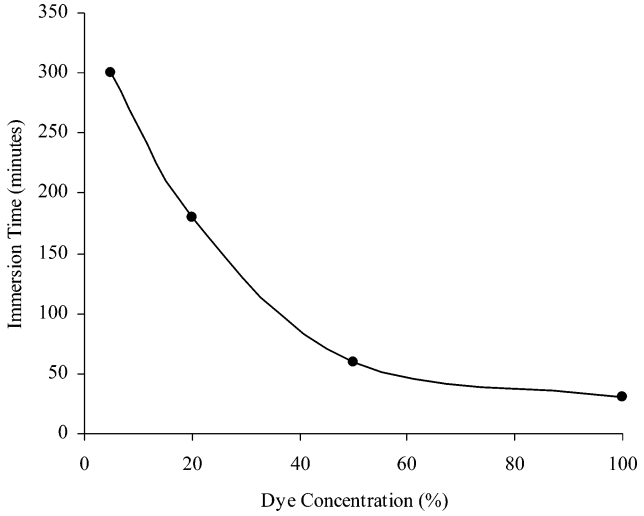

Figure 8. Plot showing the immersion time needed relative to the dye concentration for obtaining the highest efficiencies shown in each sequence for the sensitized TiO_2 film electrodes.

Figure 5 shows the SEM images of the ZnO films after sensitization in 100% dye concentration for various immersion times. It was found that an increase in the immersion time resulted in the decrease in the quality of the ZnO films. Figure 5a shows the initial ZnO film before sensitization in N3 dye, showing secondary colloidal spheres ~300 nm in diameter consisting of sintered primary nanoparticles estimated to be ~20 nm in diameter on the surface. After the immersion of the ZnO film in 100% dye concentration for 20 min, the ZnO film begins to show the formation of a layer on the surface and in between the colloidal spheres, as seen in Figure 5b. This layering may be due to the start of a reaction between the ZnO material and the solvent in the dye solution, possibly initiating the removal and deterioration of the ZnO secondary colloidal spheres and primary nanoparticles.

This can be further seen in Figure 5c, where the colloidal spheres and nanoparticles begin to merge and form a complete layer covering the individual nanoparticles and spheres after 12 h of immersion time in 100% dye concentration. The shapes of the colloidal spheres are still visible; however, the individual colloidal spheres are no longer separate. It is assumed that a continuous reaction of the ZnO material with the solvent in the dye solution caused removal of the ZnO material, forming the layer on the top surface. Figure 5d also shows further deterioration of the ZnO material after 24 h of immersion time in 100% dye concentration. It seems that the layer is completely formed, where the shapes of the colloidal spheres are no longer visible and the top layer consists of an extensive connection of sintered nanoparticles fused together. The deterioration of the ZnO film shown in the sequence of images in Figure 5 demonstrates that the stability of the ZnO film is questionable in a solvent-rich environment. The change in the quality of the film may have been the reason for the decrease in the solar cell performance of the ZnO film sensitized in 100% dye concentration with increasing immersion time. This change in film structure may have influenced the amount of dye adsorbed on the surface, thereby influencing the short-circuit current density and overall light conversion efficiency.

The change in the film quality of the ZnO film with increasing immersion time, as shown in the sequence of SEM images, may have resulted in a change in the composition of the film. However, use of XRD analysis eliminated the possibility of the presence of a different ZnO composition that may have developed from a reaction with the N3 dye solution after a prolonged amount of time. Figure 6 shows the XRD plots of the ZnO film before and after N3 dye immersion for 24 h. A comparison of the plots shows that the ZnO composition did not change after N3 dye immersion for 24 h. The (100), (002), (101), and (102) peaks representing ZnO were found before and after N3 dye immersion.

Similar instability and reactivity issues have been reported previously.[30] Horiuchi et al. found that the performance of ZnO solar cells decreased with increasing N3 dye concentration, which they attributed to the formation of aggregates. They observed that the formation of aggregates consisting of N3 dye and Zn^{2+} occurred in the ZnO film at immersion times greater than 10 min and that the electron injection from the aggregates to the ZnO films was inefficient. The presence of the aggregates

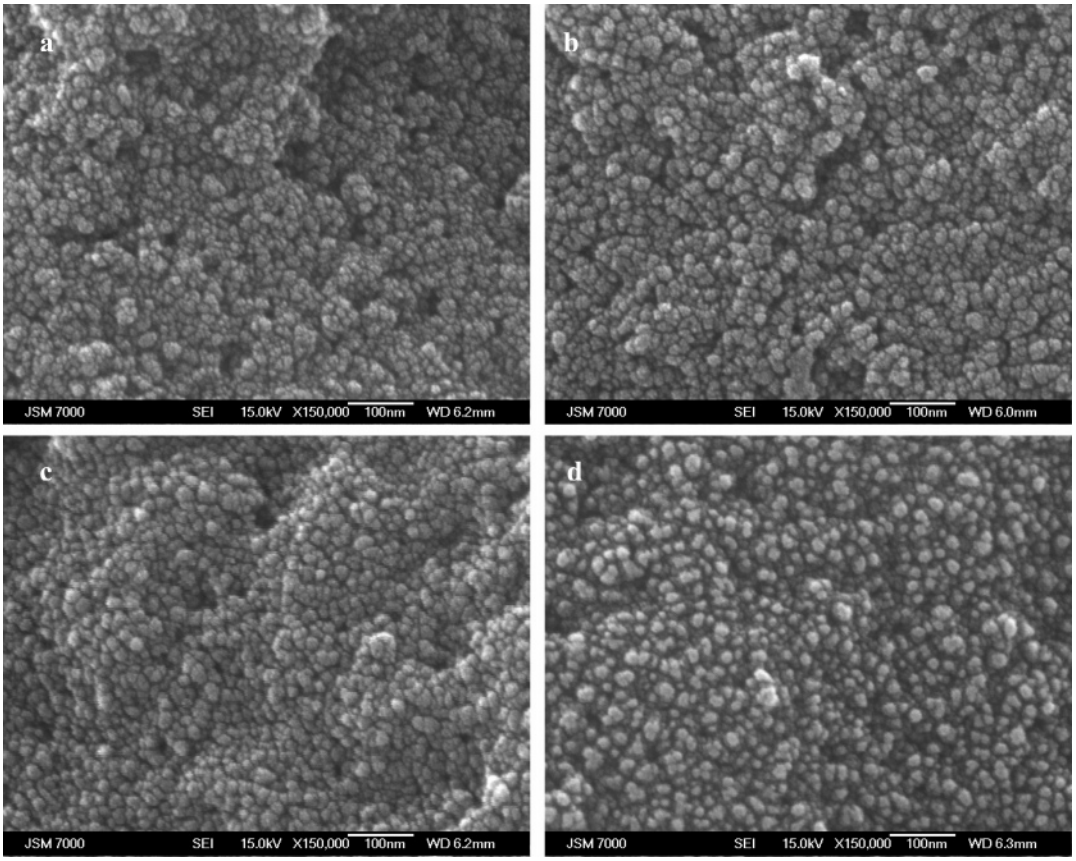

Figure 9. SEM images of TiO_2 film (a) before and (b−d) after sensitization in 100% N3 dye concentration for (b) 20 min, (c) 12 h, and (d) 24 h.

were found in the pores of the ZnO films and also presented themselves as micrometer-sized particles on the surface. It is possible that the change in film quality and surface structure of the ZnO film found in the SEM images in Figure 5 may have resulted from the aggregation of N3 dye and Zn^{2+} on the surface when immersed in high N3 dye concentration for a prolonged amount of time. In addition, the variation in the open-circuit voltage with varying immersion time and dye concentration may have also been due to the presence of N3 dye and Zn^{2+} aggregates on the surface, causing a reduction in the potential between the ZnO surface and the counter electrode.

For comparison, similar tests were performed on TiO_2 electrode films. It is assumed that since the stability of the TiO_2 material has shown to be better, prolonged immersion time in various dye concentrations would not change the solar cell performance of the sensitized TiO_2 film electrode dramatically, as seen for the sensitized ZnO film electrode. It was found that a similar trend occurred, where a higher and lower dye concentration requires a shorter and longer immersion time to obtain the maximum overall efficiency; however, the difference in the efficiencies relative to the variation in the dye concentration and the immersion time is not as dramatic as seen for the sensitized ZnO film. For the sensitized ZnO film electrodes, the maximum overall efficiencies ranged from greater than 3% down to less than 1%. For the sensitized TiO_2 film electrode, the maximum overall efficiencies ranged from greater than 3% down to greater than 1%.

Figure 7 shows the maximum overall efficiency trends at various concentrations for 30, 60, 180, and 300 min for the sensitized TiO_2 film electrodes. The trends are also illustrated in Figure 8, which correlates the required immersion time relative to the dye concentration to obtain the maximum overall efficiency found in each sequence in Figure 7. Even though a similar trend is found, as compared to that for the ZnO film electrodes, where the peak of the sequence plots representing the maximum overall efficiency is shifted to lower concentrations with increasing immersion time, the range of efficiencies correlating the dye concentration and the immersion time is smaller for the TiO_2 film electrodes.

As shown in Figure 7a, the TiO_2 film sensitized in 100% dye concentration for 30 min resulted in an efficiency of 3.13%. With decreasing dye concentration, the efficiency of the sensitized TiO_2 electrode decreased from 3.13% down to a range from 2.77% to 1.37%. In Figure 7b, the TiO_2 film sensitized in 50% dye concentration for 60 min resulted in the highest efficiency of 3.91%. A higher dye concentration of 100% resulted in a lower efficiency of 2.80%, and a lower dye concentration than 50% resulted in slightly lower efficiencies ranging from 3.04% down to 2.08%. At 180 and 300 min immersion time, as shown in their respective plots in Figure 7, parts c and d, the TiO_2 film sensitized in 5% dye concentration resulted in the highest efficiency of 3.50% and 3.77%, respectively. A higher dye concentration than 5% resulted in a lower efficiency of 3.47% down to 2.50% and 3.29% down to 2.61%, respectively.

The plot in Figure 8 shows the above-mentioned immersion time relative to the increasing trend in the dye concentration. At 100%, 50%, 20%, and 5% dye concentrations, their respective immersion times of 30, 60, 180, and 300 min were required to obtain their respective maximum overall efficiencies of 3.13%, 3.91%, 3.47%, and 3.77%. The use of shorter and longer immersion times in higher and lower dye concentrations, respectively, allowed for sufficient surface coverage of the dye molecules and thus higher efficiencies. Insufficient coverage

of dye associated with shorter and longer immersion times in lower and higher dye concentrations, respectively, resulted in lower efficiencies. In this case, the differences in the efficiencies are mainly due to the amount of dye adsorption, not necessarily the film quality. This reasoning for the sensitized TiO_2 film electrodes can further be explained by the SEM images of the films. Figure 9 shows the SEM images of the TiO_2 films before and after sensitization in 100% N3 dye concentration for various immersion times.

It can be seen that the quality and the structure of the TiO_2 film did not vary much with increasing immersion time in 100% N3 dye concentration, whereas the quality and the structure of the ZnO film varied dramatically in similar conditions, as previously shown in Figure 5. This shows that the stability of the TiO_2 film did not play a role in the resultant overall efficiency, as opposed to the ZnO film where the quality and the structure of the film, in addition to the amount of dye adsorbed, had an influence on the overall efficiency. Additional XRD analysis of the TiO_2 films also showed no change in the composition of the TiO_2 film before and after N3 dye immersion, as also shown for the ZnO films.

The above results show that the ZnO film is less stable than the TiO_2 film, as indicated in the larger difference in the $I-V$ behavior with varying dye concentration and varying immersion time, as well as the sequence of SEM images for the sensitized ZnO film, as compared to that for the TiO_2 film. The immersion time in varying dye concentrations did not affect the film quality and did not change the film structure of TiO_2. This can be attributed to the better chemical stability shown for TiO_2, when compared to ZnO, as indicated by the better overall performance of TiO_2 solar cells than that of ZnO solar cells.

There have not been any reports indicating any reactivity of TiO_2 with the N3 dye to form aggregates or precipitates, which have been reported for ZnO. Therefore, using N3 dye as the sensitizer for TiO_2 electrodes in solar cells is sufficient for efficient electron injection, whereas ZnO solar cells would require alternative sensitizers[31,32] for better electron injection efficiency and enhanced dye regeneration efficiency through the prevention of aggregate formation caused by the reactivity between the sensitizer dye and the ZnO surface.

Conclusions

It was found that the dye concentration and the immersion time greatly influenced the dye adsorption and the resultant overall light conversion efficiency of the ZnO films, which was attributed to its lower chemical stability. For a given ZnO electrode and N3 dye, the use of 100% dye concentration and 5 min immersion time offer the highest energy conversion efficiency. A similar trend was also found for the TiO_2 films; however, there was less of an influence of the N3 dye concentration and the immersion time on TiO_2 solar cells than that on ZnO solar cells. Insufficient surface coverage of dye molecules resulted from using a shorter immersion time in a lower dye concentration for both ZnO and TiO_2; however, a longer immersion time resulted in over exposure of the ZnO film in an acidic environment, possibly causing the formation of N3 dye and Zn^{2+} aggregates and/or the deterioration of the ZnO particles on the surface. A long immersion time in the dye solution did not influence the quality and structure of the TiO_2 films. The chemical stability influenced the dye adsorption and the overall light conversion efficiency of the sensitized ZnO films, whereas for the sensitized TiO_2 films, the amount of dye adsorbed was somewhat influenced by the dye concentration and the immersion time, but the stability was not an issue.

Acknowledgment. T. P. Chou acknowledges the UW−PNNL Joint Institute for Nanoscience (JIN), jointly funded by the University of Washington (UW) and Pacific Northwest National Laboratory (PNNL, operated by Battelle for the U.S. Department of Energy) and the Intel Ph.D. Foundation for their financial support. We also acknowledge the Air Force Office of Scientific Research (AFOSR-MURI, FA9550-06-1-032) for partial financial support, and Professor Samson Jenekhe and Dr. Abhishek Pradeep Kulkarni for the use of their lab and solar cell testing equipment.

References and Notes

(1) Grätzel, M. *Nature* **2001**, *414*, 338.
(2) Kaidashev, E. M.; Lorenz, M.; von Wenckstern, H.; Rahm, A.; Semmelhack, H. C.; Han, K. H.; Benndorf, G.; Bundesmann, C.; Hochmuth, H.; Grundmann, M. *Appl. Phys. Lett.* **2003**, *82*, 3901.
(3) Dittrich, Th.; Lebedev, E. A.; Weidmann, *Phys. Status Solidi A* **1998**, *165*, R5.
(4) Baxter, J. B.; Aydil, E. S. *Appl. Phys. Lett.* **2005**, *86*, 053114.
(5) Baxter, J. B.; Walker, A. M.; van Ommering, K.; Aydil, E. S. *Nanotechnology* **2006**, *17*, S304.
(6) Baxter, J. B.; Aydil, E. S. *Sol. Energy Mater. Sol. Cells* **2006**, *90*, 607.
(7) Law, M.; Greene, L. E.; Johnson, J. C.; Saykally, R.; Yang, P. *Nat. Mater.* **2005**, *4*, 455.
(8) Law, M.; Greene, L. E.; Radenovic, A.; Kuykendall, T.; Liphardt, J.; Yang, P. *J. Phys. Chem. B* **2006**, *110*, 22652.
(9) Gao, Y.; Nagai, M. *Langmuir* **2006**, *22*, 3936.
(10) Martinson, A. B. F.; Elam, J. W.; Hupp, J. T.; Pellin, M. J. *Nano Lett.* **2007**, *7*, 2183.
(11) Park, N.-G.; Kang, M. G.; Kim, K. M.; Ryu, K. S.; Chang, S. H.; Kim, D.-K.; Van de Lagemaat, J.; Benkstein, K. D.; Frank, A. J. *Langmuir* **2004**, *20*, 4246.
(12) Jiang, C. Y.; Sun, X. W.; Lo, G. Q.; Kwong, D. L.; Wang, J. X. *Appl. Phys. Lett.* **2007**, *90*, 263501.
(13) Suh, D.-I.; Lee, S.-Y.; Kim, T.-H.; Chun, J.-M.; Suh, E.-K.; Yang, O.-B.; Lee, S.-K. *Chem. Phys. Lett.* **2007**, *442*, 348.
(14) Xu, L.; Chen, Q.; Xu, D. *J. Phys. Chem. C* **2007**, *111*, 11560.
(15) Mane, R. S.; Lee, W. J.; Pathan, H. M.; Han, S.-H. *J. Phys. Chem. B* **2005**, *109*, 24254.
(16) Roh, S.-J.; Mane, R. S.; Min, S.-K.; Lee, W.-J.; Lokhande, C. D.; Han, S.-H. *Appl. Phys. Lett.* **2006**, *89*, 253512.
(17) Keis, K.; Magnusson, E.; Lindstrom, H.; Lindquist, S.-E.; Hagfeldt, A. *Sol. Energy Mater. Sol. Cells* **2002**, *73*, 51.
(18) Keis, K.; Bauer, C.; Boschloo, G.; Hagfeldt, A.; Westermark, K.; Rensmo, H.; Siegbahn, H. *J. Photochem. Photobiol., A* **2002**, *148*, 57.
(19) Nazeeruddin, M. K.; Kay, A.; Rodicio, I.; Humphry-Baker, R.; Mueller, E.; Liska, P.; Vlachopoulos, N.; Graetzel, M. *J. Am. Chem. Soc.* **1993**, *115*, 6382.
(20) Hagfeldt, A.; Grätzel, M. *Acc. Chem. Res.* **2000**, *33*, 269.
(21) Grätzel, M. *J. Photochem. Photobiol., C* **2003**, *4*, 145.
(22) Grätzel, M. *J. Photochem. Photobiol., A* **2004**, *164*, 3.
(23) Green, M. A.; Emery, K.; King, D. L.; Hishikawa, Y.; Warta, W. *Prog. Photovoltaics: Res. Appl.* **2006**, *14*, 455.
(24) Keis, K.; Lindgren, J.; Lindquist, S.-E.; Hagfeldt, A. *Langmuir* **2000**, *15*, 4688.
(25) Bauer, C.; Boschloo, G.; Mukhtar, E.; Hagfeldt, A. *J. Phys. Chem. B* **2001**, *105*, 5585.
(26) Quintana, M.; Edvinsson, T.; Hagfeldt, A.; Boschloo, G. *J. Phys. Chem. C* **2007**, *111*, 1035.
(27) Chou, T. P.; Zhang, Q.; Fryxell, G. E.; Cao, G. Z. *Adv. Mater.* **2007**, *19*, 2588.
(28) Jezequel, D.; Guenot, J.; Jouini, N.; Fievet, F. *Mater. Sci. Forum* **1994**, *339*, 152.
(29) Chou, T. P.; Zhang, Q. F.; Russo, B.; Fryxell, G. E.; Cao, G. Z. *J. Phys. Chem. C* **2007**, *111*, 6296.
(30) Horiuchi, H.; Katoh, R.; Hara, K.; Yanagida, M.; Murata, S.; Arakawa, H.; Tachiya, M. *J. Phys. Chem. B* **2003**, *107*, 2570.
(31) Otsuka, A.; Funabiki, K.; Sugiyama, N.; Yoshida, T.; Minoura, H.; Matsui, M. *Chem. Lett.* **2006**, *35*, 666.
(32) Wu, J.-J.; Chen, G.-R.; Yang, H.-H.; Ku, C.-H.; Lai, J.-Y. *Appl. Phys. Lett.* **2007**, *90*, 213109.